ELSEVIER

Journal of Structural Geology 26 (2004) 1553–1559

JOURNAL OF STRUCTURAL GEOLOGY

www.elsevier.com/locate/jsg

Rapid analysis of fold shape using Bézier curves

Deepak C. Srivastava[a,b], Richard J. Lisle[b,*]

[a]*Department of Earth Sciences, IIT Roorkee, Roorkee 247667, India*
[b]*School of Earth, Ocean and Planetary Sciences, Cardiff University, Cardiff CF10 3YE, UK*

Received 29 September 2003; received in revised form 2 February 2004; accepted 4 February 2004

Available online 11 March 2004

Abstract

We approximate and classify the forms of profile sections of folded surfaces by comparison with cubic Bézier curves. The method analyses a digital image of the fold profile, by interactive visual comparison, with the curves generated by the Bézier drawing tool available commonly in graphics software products. Simplified equations of cubic Bézier curves form the basis of the classification in terms of two parameters. The first parameter, L, is related to the distribution of curvature on a single limb of a fold between the hinge point and the inflection point. It places the fold within a shape spectrum that ranges from straight-limbed chevron folds ($L = 0$) in which curvature is concentrated in the hinge region through to rounded folds with a uniform curvature distribution ($L = 1$). The second parameter, R, is related to the ratio of amplitude to wavelength. A graph of L against R serves to group samples of folds into 'shape groups'. This classification can be used as a tool to assist the determination of relative competence of folded layers and of the folding mechanism. The new method, which has the advantages of speed and simplicity, is applied to examples of natural and experimentally developed folds to demonstrate its versatility for analysing a wide range of fold geometries.

Keywords: Fold shape; Bézier curve; Aspect ratio

1. Introduction

Folded interlayer surfaces display a broad spectrum of forms ranging from rounded geometry with a relatively uniform distribution of curvature, to straight-limbed chevron geometry with curvature concentrated in the hinge zones. Structural geologists have been long aware of the importance of fold shape attributes in the localisation of mineral resources, such as oil, gas and saddle-reef gold deposits. If these fold shape attributes can be extracted, they also might be used to help constrain kinematics and rock properties during deformation.

There are numerous previous studies concerned with the analysis and structural significance of fold shape. For example, Chapple (1969) showed that the mismatch between theoretically predicted and natural fold shapes is due to the non-linear viscous-plastic properties of rocks. Bayly (1974) related fold shape to energy dissipation during the buckling of multilayers. Woodcock (1976) used shape analysis to compare slump folds with tectonic folds and he concluded that these two types of folds are indistinguishable with respect to fold shape. Ramsay (1982) related fold shape variations, from cuspate–lobate geometry to elastica, to progressively increasing viscosity contrast. Ridley and Casey (1989) explained how the production of sharp-hinged folds could be favoured in rock layers with strong anisotropic properties. Hudleston and Lan (1994) used numerical modelling of power-law viscous materials to explore the link between fold shape and the stress exponent and the viscosity contrast between layers.

These studies have employed a number of different methods for describing and classifying fold shapes. Ramsay (1967, pp. 347–348) showed how the true-profile shapes can be distinguished using graphs that plot curvature as a function of position along the folded surface. Based on measurements of this kind, Hudleston and Lan (1994) devised a curvature index, *ki*, to assist comparison and classification of folds.

Other methods involve a comparison of the fold profile with curves corresponding to mathematical functions. For example, Chapple (1968), Stabler (1968) and Hudleston (1973a) have used Fourier analysis for quantitative

* Corresponding author. Present address: Departamento de Geología, Universidad de Oviedo, 33005, Oviedo, Spain.
E-mail address: rjlisle@geol.uniovi.es (R.J. Lisle).

0191-8141/$ - see front matter © 2004 Elsevier Ltd. All rights reserved.
doi:10.1016/j.jsg.2004.02.004

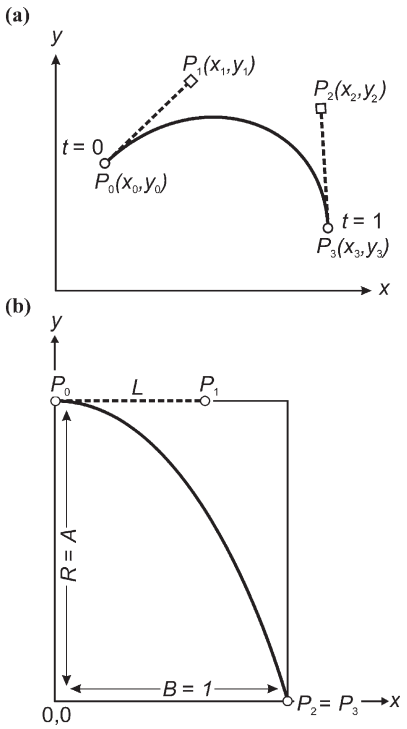

Fig. 1. (a) A cubic Bézier curve defined by four control points, P_0–P_3. The parameter t describes progress of a moving point along the Bézier curve. (b) The simplified Bézier curve used for the shape description of a fold limb. The geometry of the fold limb is scaled so that base-length B is of unit length. Consequently, A, the relative amplitude, equals the aspect ratio, R, of the fold limb. Similarly, L, the shape parameter, is equal to the distance P_1P_0.

description of fold shapes. Stabler (1968) and Hudleston (1973a) find that two Fourier coefficients are sufficient for fold classification purposes whilst Stowe (1988) advocates the use of 10 of more Fourier coefficients for accurate description of fold shapes. Other methods have employed other types of mathematical functions. For example, Bastida et al. (1999) have suggested fitting fold shapes to power functions. Their classification is based on two parameters: the exponent n, describing the shape, and the amplitude/wavelength ratio. Aller et al. (2003) utilise the eccentricity and aspect ratio of conic sections for classification of fold shapes.

To simplify the analysis of fold shape by eliminating the need for measurements of curvatures, distances or angles, Hudleston (1973a) suggested a method of classification in which the natural fold is visually compared with a series of pre-drawn standard shapes of 30 folds. These reference shapes are defined in terms of Fourier coefficients. The advantage of this technique being able to be used in the field is offset by the fact that the visual fitting is hindered by scale differences, subjectivity and a limited range of standard fold types. This paper describes a simple alternative scheme for analysing folded surfaces that takes advantage of the curve-drawing tools available on common computer drafting software. These Bézier curves can be easily designed and modified to match, by 'interactive fitting', a scanned image of most natural folds.

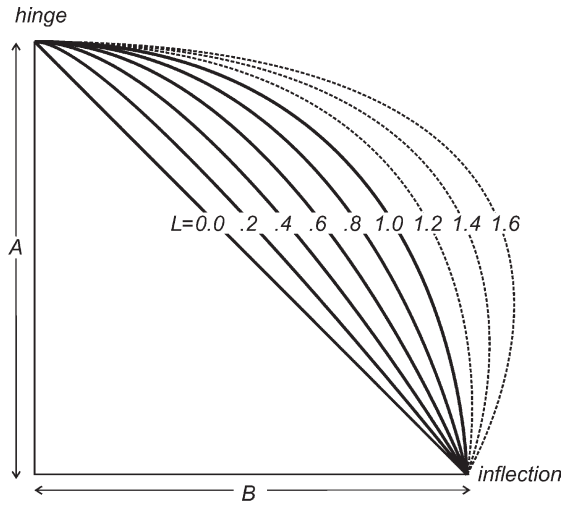

Fig. 2. Fold shapes generated by Eqs. (2a) and (2b), for unit aspect ratio, $R = 1$ (i.e. $A = B$), and various L values. Where $L > 1.0$, the interlimb angle becomes negative and the folds assumes the shapes of elastica (dashed curves).

2. Cubic Bézier curves

The present method is based on a comparison of fold profiles to cubic Bézier curves (Farin, 1990; Wojtal and Hughes, 2001). Each segment of such curves is uniquely defined by the position of four points (Fig. 1a); two points, P_0 and P_3, marking the two ends of the curve and two further control points, P_1 and P_2. The parametric equation of a segment of a cubic Bézier curve (Davies et al., 1986; De Paor, 1996) is:

$$x(t) = (1-t)^3x_0 + 3(1-t)^2tx_1 + 3(1-t)t^2x_2 + t^3x_3 \quad (1a)$$

$$y(t) = (1-t)^3y_0 + 3(1-t)^2ty_1 + 3(1-t)t^2y_2 + t^3y_3 \quad (1b)$$

The parameter t marks progress along the Bézier curve from the start point P_0, where $t = 0$, towards the end point P_3, where $t = 1$. The Bézier curve, made up of a succession of points corresponding to different t values, is therefore defined by eight quantities: (x_0, y_0), (x_1, y_1), (x_2, y_2) and (x_3, y_3), i.e. the coordinate values of points P_0, P_1, P_2 and P_3, respectively.

Since it is impractical to classify folds based on eight variables, we suggest the following procedure to reduce eight variables to two variables for describing the fold shape. Firstly, we standardise the location, orientation and scaling of the fold limb by selecting a suitable Cartesian reference frame, such that the line P_0P_1 is parallel to the x-axis and points P_0 and P_3 coincide with the hinge point and inflection point, respectively (Fig. 1b). The fold limb, at this stage, has an amplitude A, base-length B and aspect ratio $R = A/B$. Because the procedure and results are independent

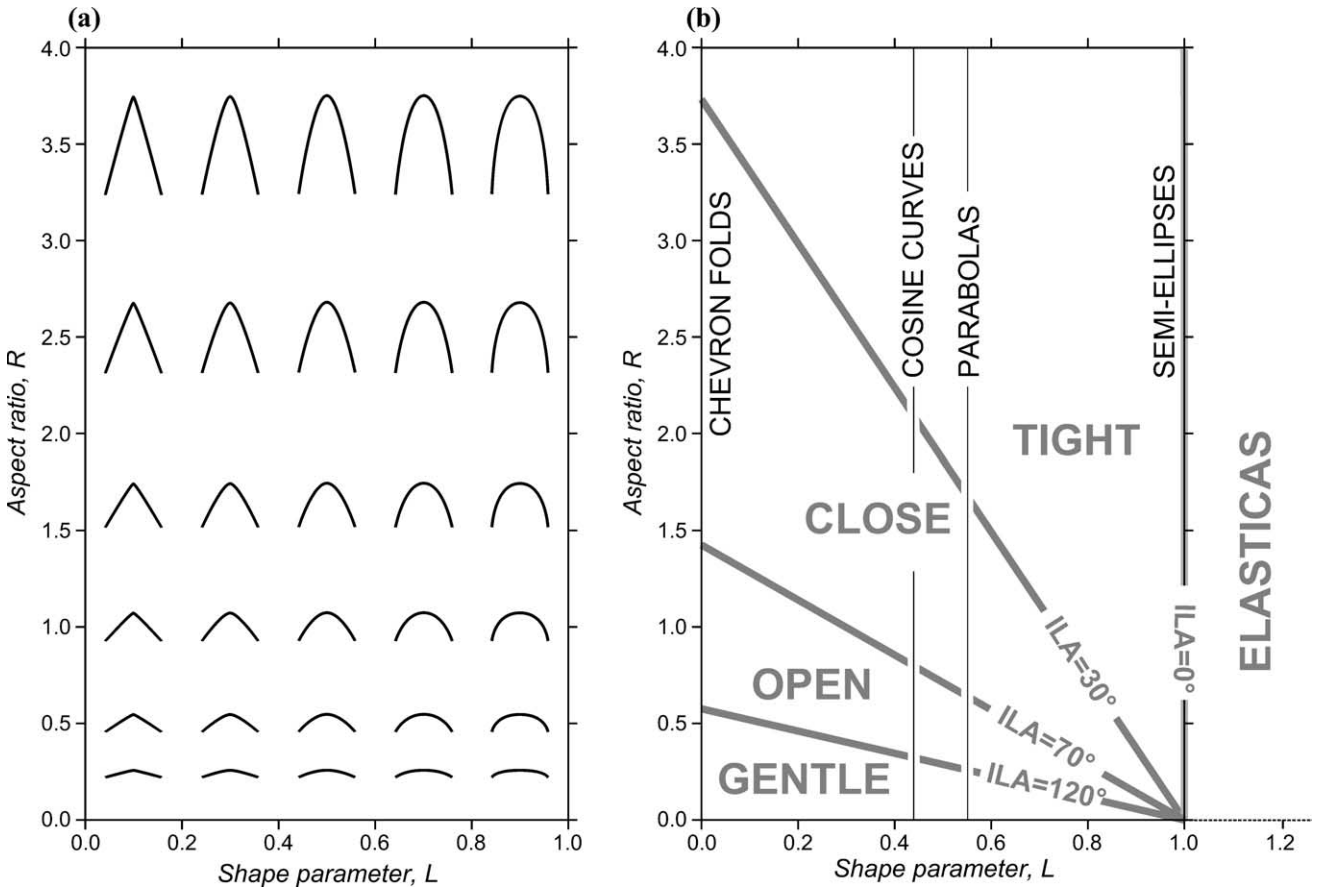

Fig. 3. (a) Fold shapes defined by L and R parameters. Most possible fold geometries can be represented on this graph. (b) Interlimb angle classification according to Fleuty (1964) and idealised fold geometries shown on the L–R diagram.

of the absolute values of A and B, we assume B to be of unit length for the sake of simplification. Secondly, we move control point P_2 to coincide with the position of P_3, so that $x_2 = 1$ and $y_2 = 0$. The effect of this is to reduce to zero the influence of P_2 on the curve's shape. The co-ordinates of points P_0, P_1 and $P_2 = P_3$ are (0, R), (L, R) and (1, 0), respectively, where L is the distance between P_0 and P_1. We define L as a fold shape parameter. By substituting the values of the new co-ordinates of P_0 (0, R), P_1 (L, R), $P_2 = P_3$ (1, 0) in Eqs. (1a) and (1b), we get the following equations of our simplified Bézier curve:

$$x(t) = 3(1-t)^2tL + 3(1-t)t^2 + t^3 \quad (2a)$$

$$y(t) = R\left\{(1-t)^3 + 3(1-t)^2t\right\} \quad (2b)$$

As a result of these simplifications to the general Bézier curve, we note that only two variables, L and R, are needed to define the fold shape and that these two variables are expressed by the position of control point P_1.

Fig. 2 shows how the shape parameter L controls the distribution of curvature in the fold limbs of unit aspect ratio. One end of the shape spectrum, $L = 0$, corresponds to chevron folds with straight limbs and curvature concentrated at the hinge. The other end member, $L = 1$, corresponds to approximately semi-circular or rounded forms where the curvature is constant, or to semi-elliptical forms depending on the aspect ratio, R. The effect of varying L and R on the fold shapes, modelled by the Bézier curves described in Eqs. (2a) and (2b), is shown in Fig. 3a. Conveniently, ideal fold geometries are characterised by L only (Fig. 3b). For example, cosine curves all possess $L = 0.44$, whilst parabolas all have $L = 0.55$. Lines of constant tightness (Fleuty, 1964), corresponding to interlimb angles possessed by equivalent symmetrical folds, are also plotted on Fig. 3b. The equation for these lines, derived by differentiating Eqs. (2a) and (2b) gives the slope of the Bézier curve at the inflection point:

$$\text{Interlimb angle} = 2\tan^{-1}\{(1-L)/R\} \quad (3)$$

Eq. (3) produces a negative slope when $L > 1$, and the corresponding fold shapes resemble elasticas (Figs. 2 and 3b). In detail, however, these curves are poorly suited for comparing with real folds because the part of these curves with greatest curvature does not coincide with the point labelled as the hinge in Fig. 2. The same problem arises with the folds that plot below the line joining the points (0,0) and (1,1) in Fig. 3a.

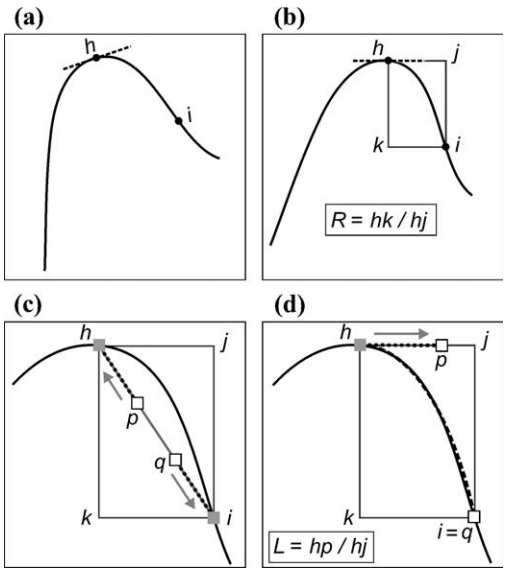

Fig. 4. Stepwise procedure for analysis of fold limb. (a) Selection of hinge point *h* and inflection point *i*. Draw tangent at hinge. (b) Rotate fold until tangent is horizontal. Points *h*, *i*, *p* and *q* correspond, respectively, to points P_0, P_3, P_1 and P_2 in Fig. 1a. (c) Move control points *p* and *q* on diagonal *hi* in direction of grey arrows (see text for details). (d) Move control point *p* from *h* towards *j* to obtain desired fit.

3. The new procedure

The new method is designed for computer implementation, and analyses a digital image of the fold's profile section taken by a digital camera or generated by scanning a photograph. Also required is a personal computer and drawing software that incorporates the cubic Bézier tool for creating curves, e.g. Corel*Draw*, Adobe *Illustrator* or Macromedia *Freehand*. The method analyses each limb of a fold separately and is therefore not limited to symmetrical folds:

(i) Import the digital image of the fold into the graphic software, say Corel*Draw*.
(ii) Mark the hinge point, *h*, and the inflection point, *i*, on the folded segment that has to be analysed, and draw a tangent at the hinge point *h* (Fig. 4a).
(iii) Rotate the image until the tangent at the hinge point becomes horizontal and draw a rectangle, *hjik*, such that line *hi* defines one of its diagonals (Fig. 4b). The aspect ratio of the fold limb, defined by the parameter *R*, equals the ratio, *hk*/*hj*, of the two sides of the rectangle.

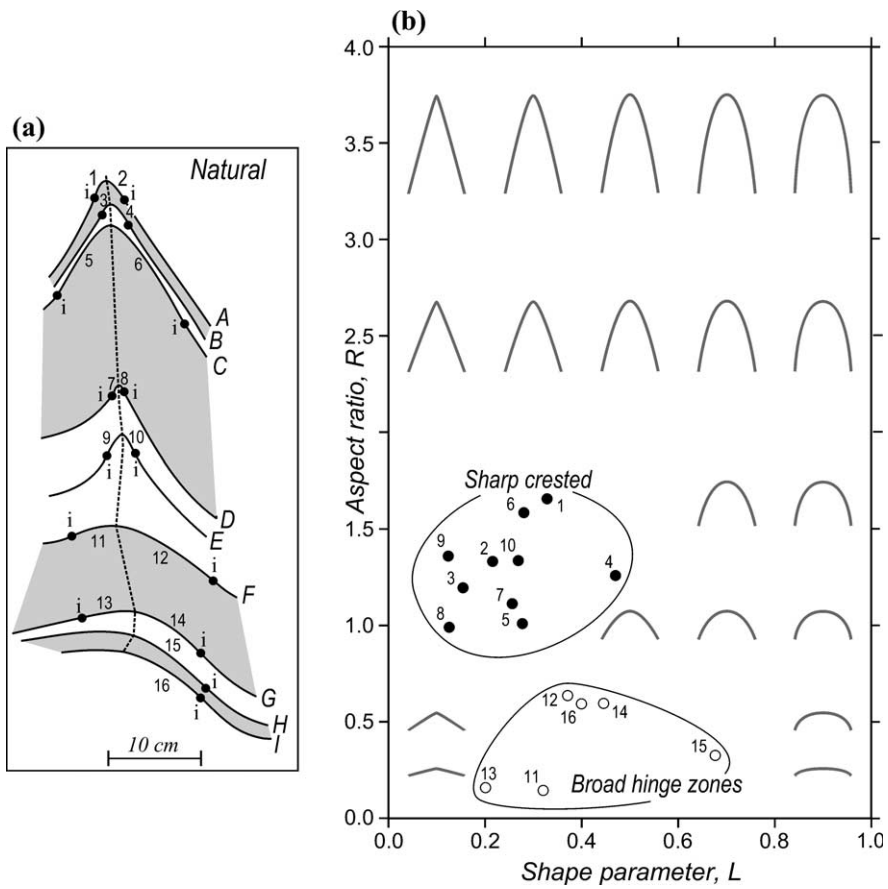

Fig. 5. (a) Example of multilayer folds in the Moine Series of Mull, Northern Scotland (after Ramsay and Huber, 1987, p. 318). Psammitic and pelitic layers are grey and white, respectively. (b) *L*–*R* plot showing results of Bézier analyses of fold limbs shown in (a). Two distinct clusters on the graph correspond to two predominant families of fold shapes present at this outcrop.

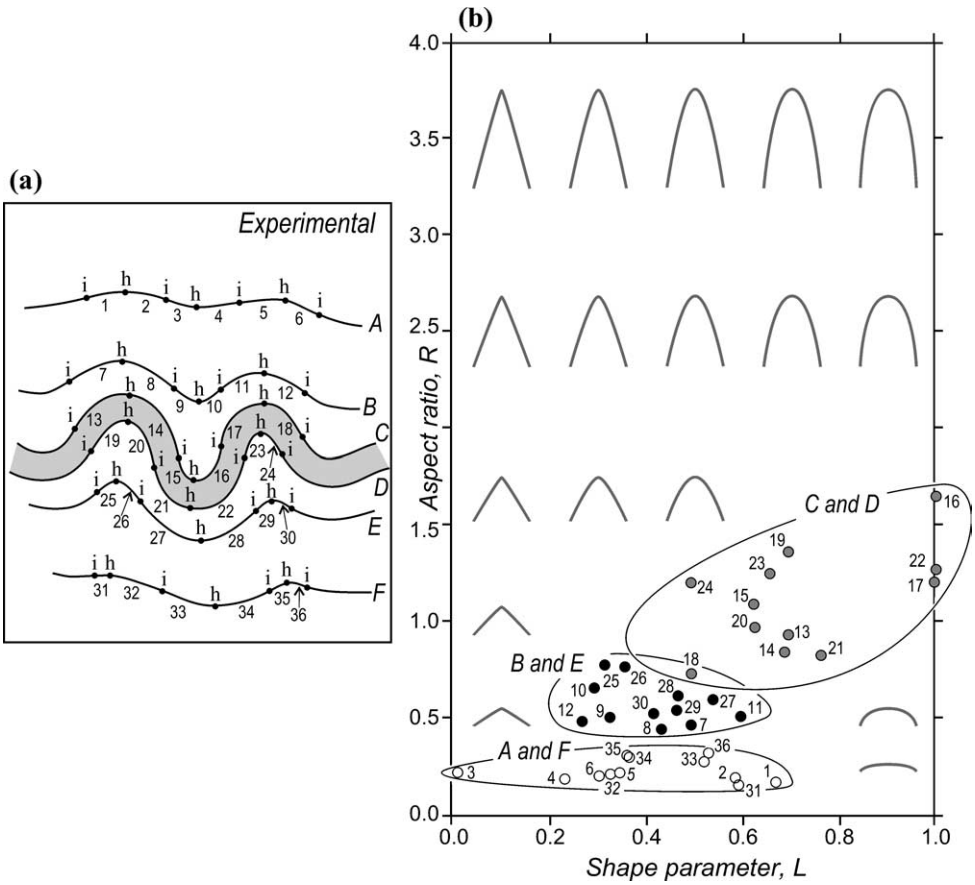

Fig. 6. (a) Shape of folds produced in single layer buckling experiment of Hudleston (1973b). The competent layer is shaded. (b) L–R plot showing results of Bézier analyses of fold limbs 1–36 shown in (a). Three clusters on the plot represent three dominant fold shapes that are correlatable to distance of the folded surface from the competent layer C–D (see text for details).

(iv) Draw a straight line, *hi* along the diagonal of the rectangle *hjik* (Fig. 4c).
(v) Convert the line *hi* into curved mode. This procedure yields two levers, *hp* and *iq*, that start from points *h* and *i* and end at two control points *p* and *q*, respectively (Fig. 4c).
(vi) Using the mouse, drag the control points *p*and *q*, such that these coincide with points *h* and *i*, respectively (Fig. 4d). Displace the control point *p* along the line *hj* until the line *hi* traces out the given fold shape. The shape parameter L is given by the ratio *hp*/*hj* (Fig. 4d).
(vii) Plot R and L as a point on the Cartesian graph shown in Fig. 3. This point uniquely defines the shape of the given fold limb. Mathematically, the shape of the limb is described by Eqs. (2a) and (2b) by substitution of values of L and R and varying t from 0 to 1.

4. Examples

The Bézier curve method has been tested on a large number of scanned images of idealised fold shapes (figs. 12 and 13 in Hudleston, 1973a), experimentally simulated fold shapes (figs. 3 and 8 in Hudleston, 1973b) and natural occurrences of folds (fig. 2 in Stabler, 1968; figs. 15.15 and 19.11 in Ramsay and Huber, 1987, pp. 318 and 393; fig. 2 in Lisle, 1992). Bézier curves satisfactorily matched all the examples, except for a series of five box folds depicted in figs. 1A–5A in Hudleston (1973a). Box folds and multiple hinge folds, in general, are difficult to simulate by Bézier curves because of the lack of inflection points between successive hinges. For the purpose of illustration of the new method, we present only two examples here; one of natural fold shapes and one of experimentally produced folds.

4.1. Multilayer folds in Moine Series from Mull, Scotland

This example, taken from part of fig. 15.15 in Ramsay and Huber (1987, p. 318), shows a variety of fold shapes traced by the psammite–pelite sequence. In addition to inflection points, hinge points and axial traces, different limbs of folded layers are marked from 1 to 16 (Fig. 5a). Each limb is analysed separately by using the Bézier method and plotted as a point on the Cartesian graph L–R (Fig. 5a). These points fall in two distinct clusters that imply the occurrence of two dominant families of fold shapes at this outcrop. The cluster corresponding to relatively smaller values of L and higher values of R encloses plots of

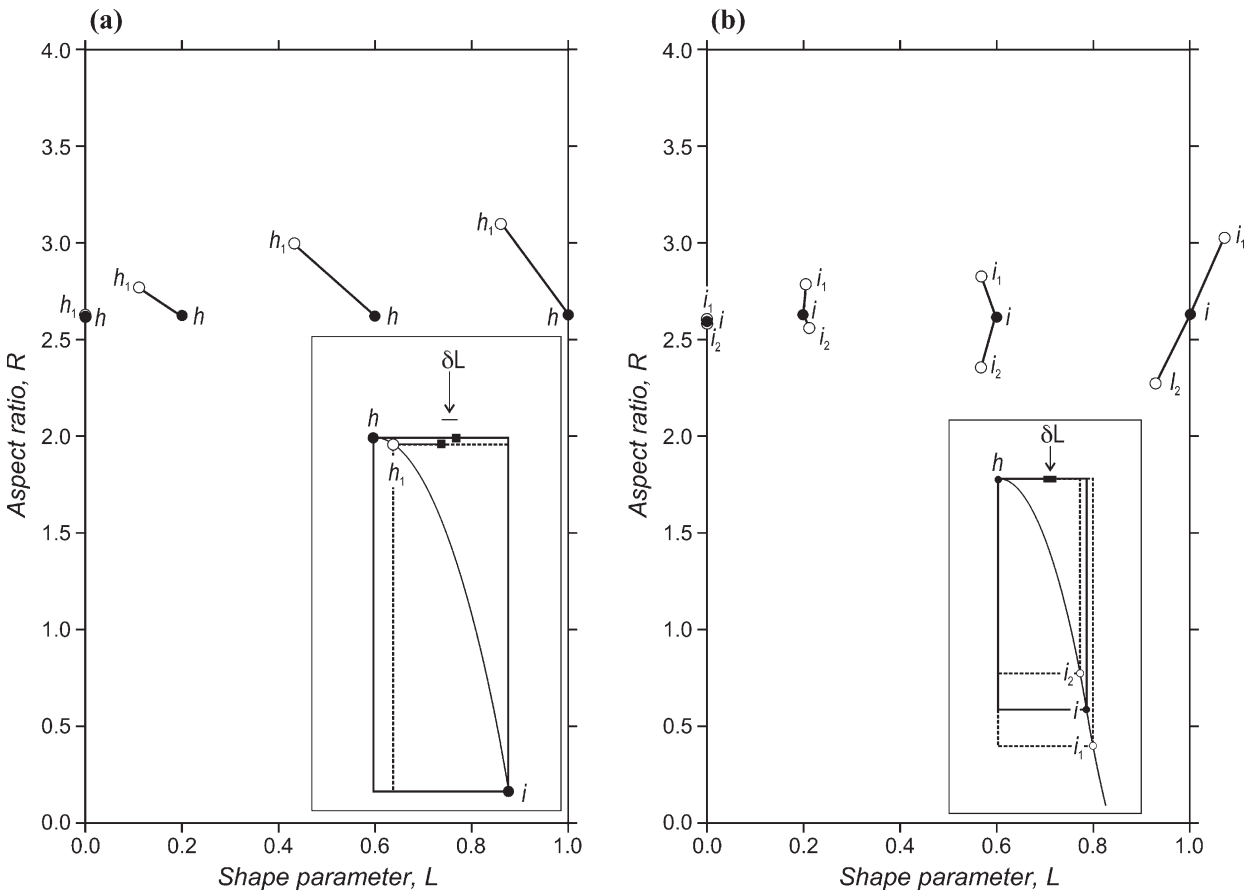

Fig. 7. Errors in selection of hinge and inflection points. These estimates are depicted for folds with correct aspect ratio $R = 2.6$. (a) h—correct hinge point, h_1—hinge point offset by 15% of the quarter wavelength of fold. Tie lines join the plots for four folds corresponding to $L = 0.0$, 0.2, 0.6 and 1.0, respectively. Inset shows an example of fold with $L = 0.6$. δL—deviation in control point due to offset of hinge point from h to h_1. (b) i—correct inflection point. i_1 and i_2—inflection points with a shift of $\pm 15\%$ of the linear distance between hinge point h and correct inflection point i, respectively. Inset shows an example of fold with $L = 0.6$. δL—deviation in control point due to shift in inflection point from i_1 to i_2.

sharp-crested folds with relatively higher amplitude/wavelength ratios. The second cluster, corresponding to higher values of L and smaller values of R, contains plots of broad hinge zone folds with relatively lower amplitude/wavelength ratios (Fig. 5b).

4.2. Experimental folds

This example is based on folds developed in a single layer buckling experiment of Hudleston (1973b). The folds shown in Fig. 6a consist of six surfaces; namely, A–F. Surfaces C and D bound an active competent layer, whilst all other surfaces are analogous to passive layers.

Results of Bézier curve analyses on 36 fold limbs in layers A–F are plotted on an L–R graph, where three clusters are evident (Fig. 6b). These clusters correspond to a position of the folded surface with respect to the competent layer C–D and its zone of contact strain. The competent layer (C–D) shows folds of relatively high amplitude, and shapes between parabola and semi-ellipse. Adjacent to the competent layer (B and E), the folds show smaller amplitude and shapes similar to cosine curves. Farther from the competent layer (A and F), an amplitude decrease is associated with folds with a range of shapes including those approaching chevron style.

5. Limitations and sources of error

The method proposed here is not suitable for multiple hinge folds. Bézier curves tend to fit rather poorly to very broad hinged folds and folds with limb dip greater than 90°, e.g. elastica folds. Although the method is not free from measurement errors, these can be minimised by using graphic tools, such as ‘snap to guidelines’ in Corel*Draw*.

The analysis of fold shapes by Bézier curves is, however, sensitive to the selection of hinge and inflection points on the folded layer. The errors in the results, in general, increase with the roundness of the hinge zone; chevron folds are least affected and semi-circular or semi-elliptical folds are most affected. We demonstrate these effects with the help of four idealised fold shapes, all with an aspect ratio of $R = 2.6$, but with a shape parameter L equal to 0.0, 0.2, 0.6 and 1.0, respectively. A shift in the hinge point by an

amount equal to 15% of the quarter-wavelength of the fold results in a considerable increase in crest sharpness (decrease in L) and also an increase in the determined aspect ratios of all folds (Fig. 7a). Similarly, an error in locating inflection points, by an amount equal to $\pm 15\%$ of the linear distance between hinge point and inflection point (hi), results in a significant change in aspect ratio, but in a relatively minor change in the shape of the folds (Fig. 7b). The aspect ratio increases or decreases depending upon the direction in which the inflection point is shifted.

We emphasise that the method described here, in common with all related methods, is designed for the analysis of true fold profiles. Oblique sectioning can lead to large errors, depending on the deviation of the section plane from the profile plane.

6. Conclusions

Computer-aided Bézier curve analysis offers a quick method for analysing the distribution of curvature from the hinge point to the inflection point in any segment of a folded surface. With some practice, it takes only a few minutes to analyse a given fold limb. Since our method analyses individual fold limbs, its application is independent of the symmetry of the folds (Twiss, 1988).

An advantage of the present method over other methods that match folds with mathematical functions is that the fitting procedure involves the use of the entire curve, rather than the coordinates of a few selected points. The results can be conveniently plotted on the L–R graph in Fig. 3, where L and R are parameters expressing the fold's curvature distribution and aspect ratio, respectively. Tests on several natural, experimental, and idealised examples demonstrate the practicality and speed of the method and its applicability to a large variety of possible fold forms.

The new method serves to separate folds, observed at the outcrop or simulated in numerical or analogue experiments, into 'shape groups'. We provide an example where such groupings may be interpreted in terms of the location of folds within the zone of contact strain in the vicinity of a buckled competent layer (Fig. 6). There are, however, several other uses of this shape analysis tool. For example, the method may find application in attempts to distinguish folds in terms of modes of formation (e.g. layer parallel shortening, diapirism, syn-sedimentary slumping, tectonic deformation of indurated layers), in terms of relative layer competence, or in terms of folding mechanisms.

Acknowledgements

The idea to use Bézier curves for fold classification arose out of discussions with Cees Passchier. DCS thanks the Association of Commonwealth Universities for funding his visit to Cardiff University. Sue Treagus and Scott Wilkerson provided useful reviews.

References

Aller, J., Bastida, F., Toimil, N.C., Bobillo-Ares. N.C., 2004. The use of conic sections for the geometrical analysis of folded profile surfaces. Tectonophysics, 379, 239–254.

Bastida, F., Aller, J., Bobillo-Ares, N.C., 1999. Geometrical analysis of folded surfaces using simple functions. Journal of Structural Geology 21, 729–742.

Bayly, M.B., 1974. An energy calculation concerning the roundness of folds. Tectonophysics 24, 291–316.

Chapple, W.M., 1968. A mathematical theory of finite-amplitude rock-folding. Geological Society of America Bulletin 79, 47–68.

Chapple, W.M., 1969. Fold shape and rheology; the folding of an isolated viscous-plastic layer. Tectonophysics 7, 97–116.

Davies, B.L., Robotham, A.J., Yarwood, A., 1986. Computer-aided Drawing and Design, Chapman and Hall, London, 328pp.

De Paor, D.G., 1996. Bézier curves and geological design. In: De Paor, D.G., (Ed.), Structural Geology and Personal Computers, Pergamon Press, pp. 389–417.

Farin, G.E., 1990. Curves and Surfaces for Computer Aided Geometric Design: a Practical Guide, 2nd Ed, Academic Press, Boston, 444pp.

Fleuty, M.J., 1964. The description of folds. Proceedings of the Geologists Association 75, 461–492.

Hudleston, P.J., 1973a. Fold morphology and some geometrical implications of theories of fold development. Tectonophysics 16, 1–46.

Hudleston, P.J., 1973b. An analysis of 'single layer' folds developed experimentally in viscous media. Tectonophysics 16, 189–214.

Hudleston, P.J., Lan, L., 1994. Rheological controls on the shapes of single-layer folds. Journal of Structural Geology 7, 1007–1021.

Lisle, R.J., 1992. Strain estimation from flattened buckled folds. Journal of Structural Geology 14, 369–371.

Ramsay, J.G., 1967. Folding and Fracturing of Rocks, McGraw-Hill, New York, 568pp.

Ramsay, J.G., 1982. Rock ductility and its influence on the development of tectonic structures in mountain belts. In: Hsu, K., (Ed.), Mountain Building Processes, Academic Press, London, pp. 111–127.

Ramsay, J.G., Huber, M.I., 1987. The Techniques of Modern Structural Geology. Volume 2. Folds and Fractures, Academic Press, New York, pp. 309–700.

Ridley, J., Casey, M., 1989. Numerical modelling of folding in rotational strain histories: strain regimes expected in thrust belts and shear zones. Geology 17, 875–878.

Stabler, C.L., 1968. Simplified Fourier analysis of fold shapes. Tectonophysics 6, 343–350.

Stowe, C.W., 1988. Application of Fourier analysis for computer representation of fold profiles. Tectonophysics 156, 311–333.

Twiss, R.J., 1988. Description and classification of folds in single surfaces. Journal of Structural Geology 10, 607–623.

Wojtal, S., Hughes, G., 2001. Using Bézier curves to analyze the shapes of folded surfaces. Abstracts with Program—Geological Society of America 33(6), 26.

Woodcock, N.H., 1976. Structural style in slump sheets: Ludlow Series, Powys, Wales. Journal of the Geological Society of London 132, 399–415.